This chapter is mainly focused on modification inserts chelating characteristics for polymeric resin (modified chelating resin, MCR), which may be used to bind metal ions from external matrices and characterized using FTIR, SEM-EDX.

3.1. Introduction

Aqueous bodies are most valuable and essential components on the earth. Unfortunately, quality of water resources is deteriorating day by day due to growth in population/civilization, domestic sewage, agricultural activities, industrialization, geological and climate changes [1,2]. The important environmental issue for water pollution is the presence of heavy metal ions (cobalt, nickel, copper, zinc, cadmium, mercury and lead) coming from various industries sources release wastewater containing metal or metal derivatives [3,4]. Heavy metal toxicity is caused by these metal ions, which are harmful even at extremely low concentrations and are not biodegradable chemically or biologically [5–9]. Among various processes, ion exchange is one of the most effective and simple available process for the removal of transition and heavy metal ions from waste water [10,11]. An extensive literature is available on types of adsorbents (activated carbons) [12], surface modified zeolites [13], graphene oxide and its composites [14], biosorbents [15], tetravalent metal phosphonate [16] and chelating materials [17]) utilised for the removal of metal ions. A few studies, using ion exchange resins such as Duolite GT-73, Lewatit TP 207, Lewatit CNP 80, and Amberlite IRA-420, have also been reported [18–20].

The exchange/adsorption property of the adsorbents depends upon the functional groups present on their surfaces [21]. Functional groups such as carboxylic [22], phenolic, amide and amine [23] provide binding sites for metal ions. The donor atom of functional groups behaves as Lewis base, which forms co-ordinate bond with heavy metal ion, which acts as Lewis acid [24]. However, polymeric resin has not been modified with the point of view of insertion of chelating capacity in the resin, which can potentially be used for binding/exchange of metal ions.

The aim of the work is to examine the removal of metal ions by using commercially available polymeric resin (Amberlite IRA-400(Cl^-)). In the present study, the resin has been modified with disodium salt of ethylene diamine tetra acetic acid (Na_2EDTA). This modification inserts chelating characteristics in the above polymeric resin (modified chelating resin, MCR), which may be used to bind metal ions from external matrices. MCR may show chelating properties due to presence of two –COOH groups and two >N- groups. –COOH

groups are responsible for exchange of metal ions with H^+ of carboxylic group and simultaneously imine groups bind with metal ions [Transition metal (Co^{2+}, Ni^{2+}, Cu^{2+}, Zn^{2+}) and heavy metal (Cd^{2+}, Hg^{2+}, Pb^{2+})] through co-ordinate bonds. Na_2EDTA behaves as tetra dentate chelating ligand. This incorporates effect of complexing agent in the MCR and responsible for separating metal ions from background solution [8]. The MCR was characterized by EDX, SEM and FTIR. In aqueous and various electrolyte media/concentration, distribution coefficients (K_d) of metal ions [Transition metal (Co^{2+}, Ni^{2+}, Cu^{2+}, Zn^{2+}) and heavy metal (Cd^{2+}, Hg^{2+}, Pb^{2+})] have been computed by batch equilibrium technique. Effect of pH has also been seen on the exchange process. The Langmuir and Freundlich adsorption models have been applied at various fixed temperatures and different concentrations of the exchanging metal ions. Thermodynamic parameters, equilibrium constant (K), standard Gibbs free energy (ΔG°), enthalpy (ΔH°), and entropy (ΔS°) changes, were evaluated by temperature dependence of the exchange process. Kinetic study, for exchange of metal ion, was performed to obtain information related to mode of kinetic exchange. Elution behavior of above metal ions has also been seen using various acids and electrolyte by adopting column method.

3.2. Experimental section

All the chemical materials, methods and physical measurements utilized in this work are comprehensively interpreted in the “Chapter 2” (Section 2.1, 2.2 and 2.4).

3.2.1. Distribution study

The distribution coefficient (K_d) was evaluated by batch method for the transition and heavy metal ions (Co^{2+}, Ni^{2+}, Cu^{2+}, Zn^{2+}, Cd^{2+}, Hg^{2+} and Pb^{2+}) by taking 0.1 g of the MCR, equilibrated with 10 mL of 0.001 M to 0.007 M of all metal solutions (for different durations (15, 30, 45, 60, 75, 90, 105, 120, 150 min and upto 24 h)) at room temperature. Concentration of the metal ion was determined by using complexometry titration before and after sorption on the MCR. The K_d value was also evaluated at optimum condition with 0.1 g of the exchanger in aqueous as well as in presence of various electrolytic media [nitric acid (HNO_3), perchloric acid ($HClO_4$), acetic acid (CH_3COOH), ammonium nitrate (NH_4NO_3)] for two different metal concentrations (0.02 and 0.2 M) at room temperature. K_d values have been calculated using Eq. (1) [25].

$$K_d = \frac{(I-F)}{F} \times \frac{V}{W} \quad (1)$$

where I is the initial [metal ion] solution, F is the final [metal ion] solution, W is the weight of the exchanger in gram and V is the volume of the metal ion solution in mL.

3.2.2. Adsorption studies

3.2.2.1. Effect of pH, contact time and temperature on adsorption/ion exchange

Adsorption of transition and heavy metal ions (Co^{2+}, Ni^{2+}, Cu^{2+}, Zn^{2+}, Cd^{2+}, Hg^{2+} and Pb^{2+}) has been carried out by MCR shaking 0.1 g MCR with 10 mL of 0.002 M metal ion solution under adjusted pH (1–7) by using pH meter. The decanted solution was used to determine quantity of the transition and heavy metal ion by complexometry titrations [26]. The percentage uptake was calculated using the following expression:

$$\frac{(C_0 - C_e)}{C_0} \times 100 \quad (2)$$

where C_0 and C_e are the initial and final concentrations of metal ion in mg/L, respectively. This experiment was performed in a temperature range of 299–329 K with a 10-K interval.

3.2.3. Thermodynamic studies

3.2.3.1. Equilibrium time determination

It is determined with 0.1 g of MCR, which was shaken with 10 mL of 0.002 M metal ion solution in a stoppered conical flask (varying time from 15 min to 24 h). After each time interval, the mixture was decanted and the metal ion concentration in the solution was determined by complexometry titration. A plot of the fractional attainment of equilibrium (U(t)) vs. time (t) for exchanged metal. This shows that an equilibrium has been attained within 120 min (optimum equilibrium time).

3.2.3.2. Equilibrium experiments

In these experiments, 0.1 g of MCR, at different temperatures (299–329 K with a 10 K interval), shaked with 20 mL of a mixture of solution (containing 0.06 M HCl and 0.02 M metal ion solution (1, 3, 5, …, 19 mL of 0.02 M metal ion solution and 19, 17, 15, …, 1 mL of 0.06 M HCl), After each time interval, metal ion concentration was determined by complexometry titration.

Temperature dependent data have been used to obtain thermodynamic parameters such as equilibrium constant (K), standard Gibbs free energy ($\Delta G°$), entropy ($\Delta S°$) and enthalpy ($\Delta H°$) changes [27].

3.2.4. Sorption kinetics

The kinetics of sorption of MCR was investigated using the pseudo-first-order, pseudo-second-order and intraparticle diffusion reaction models.

3.2.4.1. Pseudo-first-order kinetic model

The kinetic model can be given by Eq. (3) [28].

$$log(q_e - q_t) = logq_e - (\frac{K_1}{2.303})t \quad (3)$$

where q_t and q_e are the amount of solute adsorbed per g of sorbent (mg/g) at certain time (t) and at equilibrium, respectively. K_1 is the rate constant of pseudo-first-order sorption (min^{-1}). The straight-line plot of of log ($q_e - q_t$) against t gives log (q_e) as slope and $K_1/2.303$ as intercept.

3.2.4.2. Pseudo-second-order kinetic model

The model is represented by Eq. (4) [29]:

$$\frac{t}{q_t} = \frac{1}{K_2 q_e^2} + \frac{t}{q_e} \quad (4)$$

where K_2 is the rate constant of pseudo-second-order sorption (g/mg min) and q_e values are calculated from the slope of the straight line. The plots of t/q_t vs. t (straight lines) the slope and intercept are $1/q_e$ and $1/K_2 q_e^2$, respectively.

3.2.4.3. Weber-Morris intraparticle diffusion model

The expression for the Weber–Morris intraparticle diffusion model is represented by Eq. (5) [30].

$$q_t = K_{id} t^{1/2} + C \quad (5)$$

where K_{id} is the intraparticle diffusion rate constant (mg/g $min^{1/2}$) and C (mg/g) is the intercept. K_{id} can be obtained by the plot of q_t vs. $t^{1/2}$.

3.2.5. Elution studies

Elution studies were performed by taking 0.5 g of MCR in a column followed by washing with de-ionized water (flow rate 0.5 mL/min). Metal ion (Co^{2+}, Ni^{2+}, Cu^{2+}, Zn^{2+}, Cd^{2+}, Hg^{2+} and Pb^{2+}) has been determined quantitatively by complexometry titration. For such study (single metal), column was prepared. The metal ion solution (0.002 M, 10 mL) was loaded to the column. The metal ion loaded column was eluted with eluents such as HNO_3, $HClO_4$, CH_3COOH and NH_4NO_3 (0.02 M or 0.2 M). The % of metal ion eluted (% E) was calculated using Eq. (6).

$$\%E = \frac{C_e}{C_0} \times 100 \quad (6)$$

where C_e is the amount of metal ion in the eluted solution and C_0 is the amount of metal ion present in the loaded solution.

3.3. Result and discussion

Amberlite IRA-400(Cl^-) resin is a strongly basic, anion exchange resin. Chloride ion is associated with tertiary nitrogen of amine group by electrostatic bond. When, Amberlite IRA-400(Cl^-) resin was shaked with 0.01 M solution of Na_2EDTA for 24 h. Chloride ion was completely substituted with $EDTA^{2-}$ and substitution of Cl^- was confirmed by EDX analysis. The resultant MCR was obtained as reddish brown translucent spherical beads or granules and insoluble in water. The MCR contains two nitrogen of amine group and two oxygen of carboxylic group, offering chelating sites to metal ion and behave as cation exchange unit. The structure of metal-loaded MCR has been shown in **Figure 3.1**.

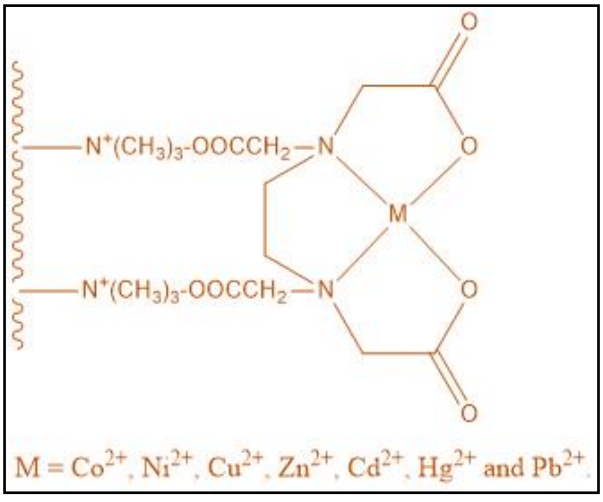

Figure 3.1. Schematic Structure of metal loaded MCR.

3.3.1. SEM-EDX

Surface morphologies for pure and modified were investigated by SEM analysis **(Figure 3.2 (a and b))**. This study shows that no significant modification in surface morphology takes place on the insertion of chelating moiety (i.e., Na_2EDTA). This reveals that chelating moiety binds at the surface of the resin and does not affect internal resin structure and hence morphology. EDX spectra of Amberlite IRA-400(Cl^-) resin, MCR, transition metal (Zn^{2+}) loaded MCR and heavy metal (Pb^{2+}) loaded MCR are illustrated in **Figure 3.3 (a-d)**. Absence of Cl^- ion in the MCR indicates that Cl^- ion has been removed by $EDTA^{2-}$. Presence of Co^{2+}, Ni^{2+}, Cu^{2+}, Cd^{2+} and Hg^{2+} metal ions in the images of metal-loaded MCR and tables of EDX also revealed uptake of metal ions by modified resin as shown in **Figure 3.4 (a-c) and Figure 3.5 (a and b)**.

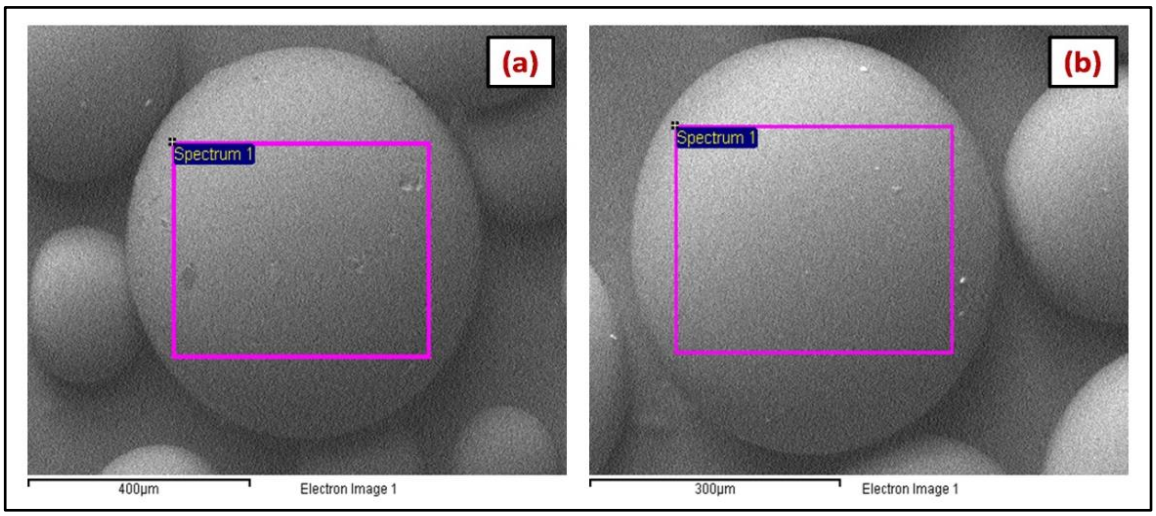

Figure 3.2. SEM micrographs of (a) Amberlite IRA-400(Cl^-) resin and (b) MCR.

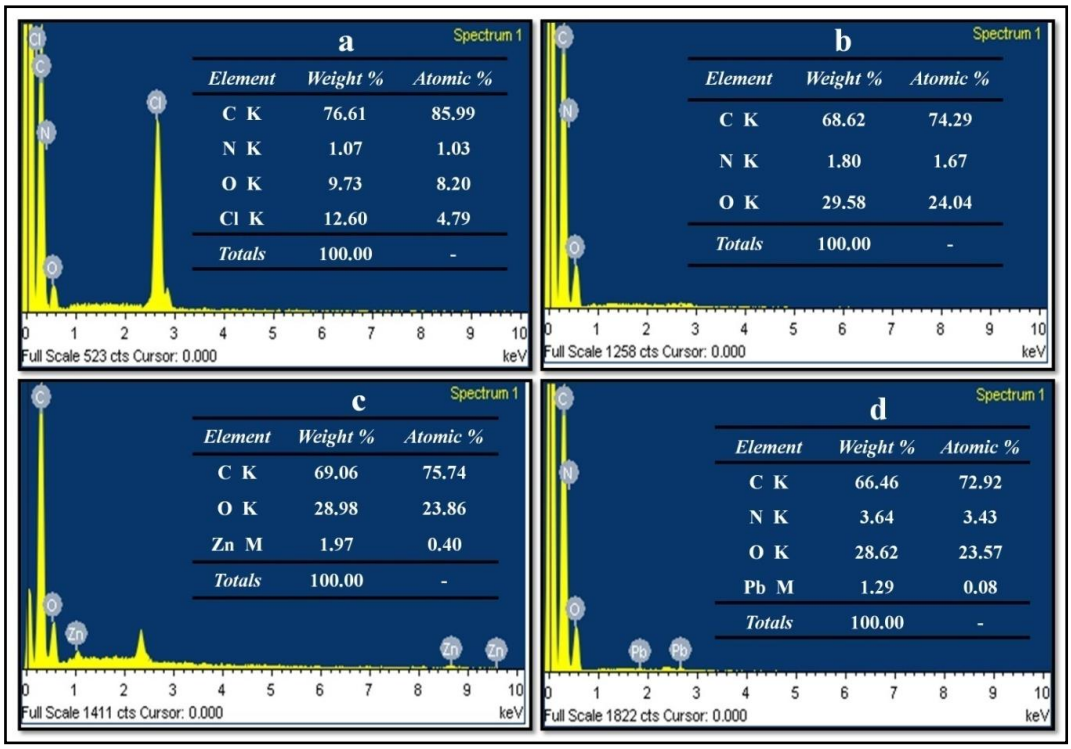

Figure 3.3. EDX spectra of (a) Amberlite IRA-400(Cl^-) resin, (b) MCR, (c) Zn^{2+} loaded MCR and (d) Pb^{2+} loaded MCR.

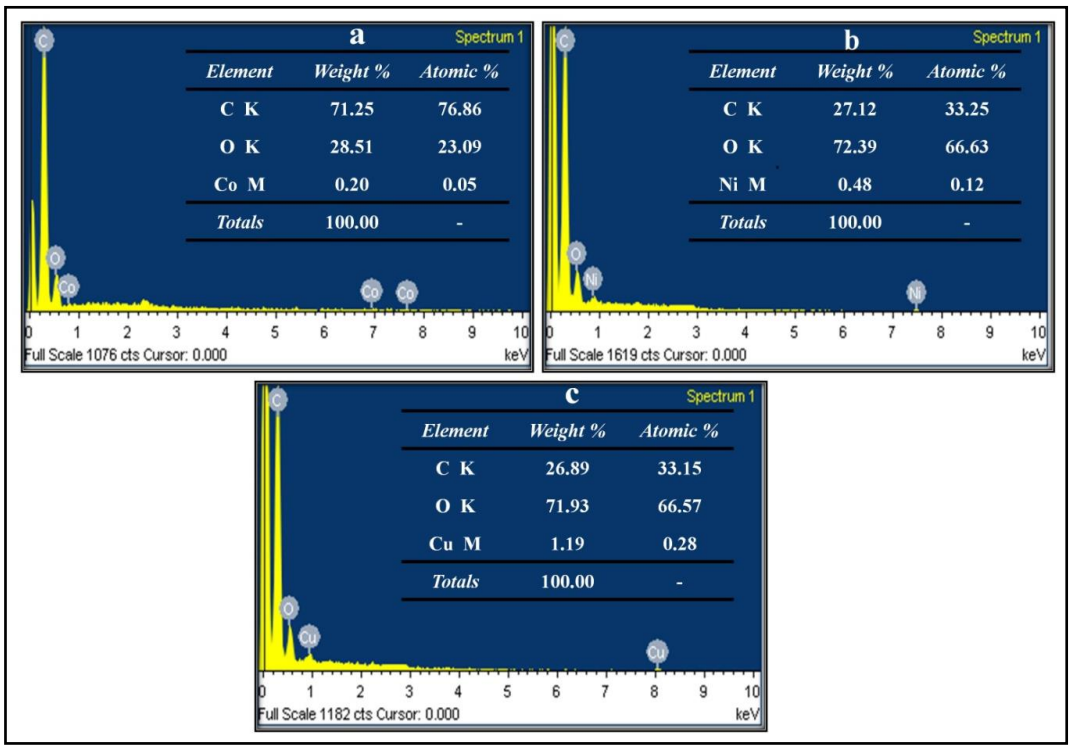

Figure. 3.4. EDX spectra of (a) Co^{2+} (b) Ni^{2+} (c) Cu^{2+} loaded MCR.

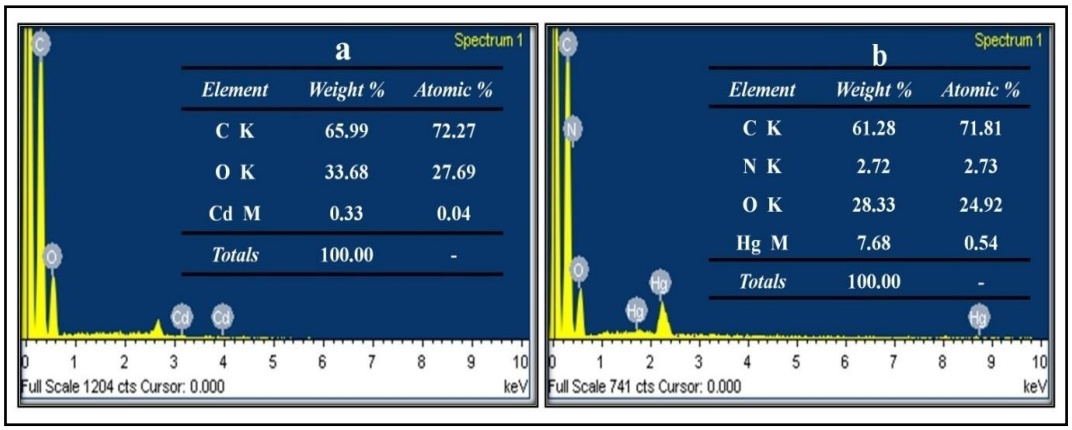

Figure. 3.5. EDX spectra of (a) Cd^{2+} (b) Hg^{2+} loaded MCR.

3.3.2. FTIR

FTIR absorption spectrum of sample Amberlite IRA-400(Cl^-) resin, modified Amberlite IRA-400(Cl^-) resin (MCR), and Pb^{2+} metal-loaded MCR is presented in **Figure 3.6**. FTIR spectra show a broad bend in the 400–4,000 cm^{-1} range. A sharp medium band at 1,690 cm^{-1} is attributed to –C=O stretching vibrations in the modified Amberlite IRA-400(Cl^-) resin. It is a confirmation of the modification of Amberlite IRA-400(Cl^-) resin with disodium salt of EDTA. The absorption peak 1,690 cm^{-1} is also observed in metal-loaded MCR. The O–H bending vibration is observed at 1,408 cm^{-1} in MCR and it shifted to 1,411 cm^{-1} after metal-loaded MCR. The absorption peak observed at 1,220 cm^{-1} is due to (C–N) in MCR, which shifted to 1,232 cm^{-1} in metal-loaded MCR. The metal ion has positive character when it is attached with coordinating sites of modified resin and attracts electron density. So, energy of bands are changed and small peaks get merged and converts into an intense band in FTIR spectrum **(Figure 3.6)**.

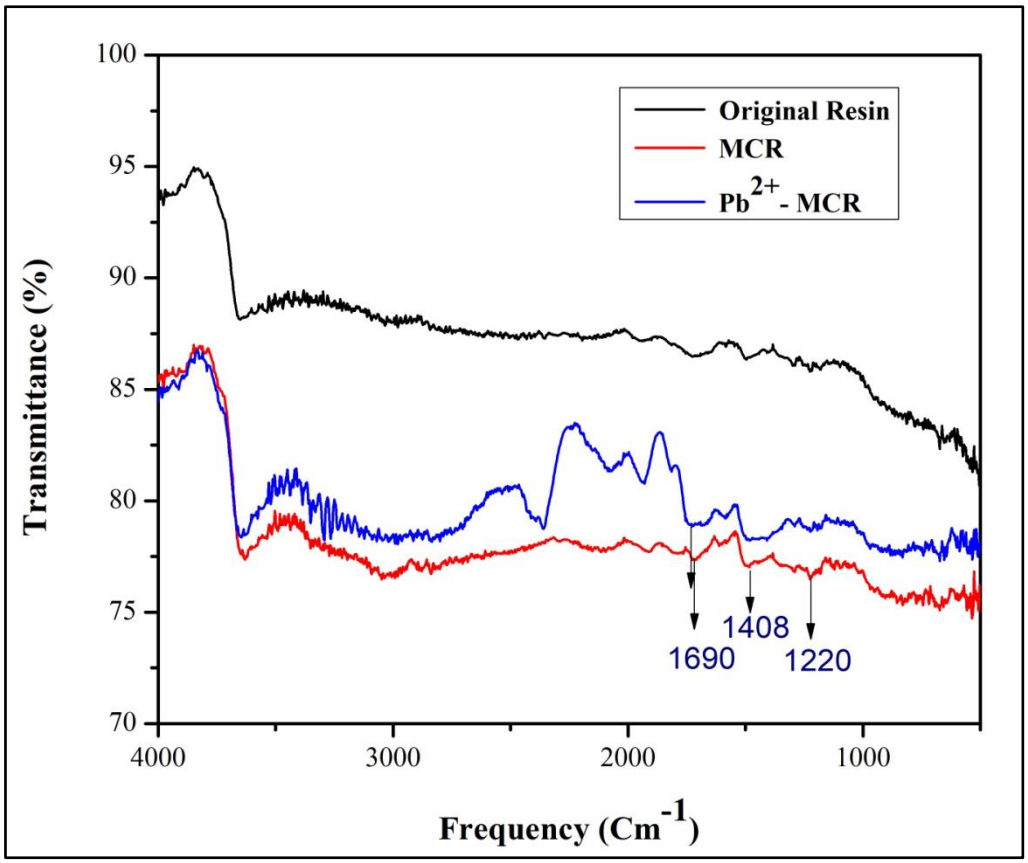

Figure 3.6. FTIR of Amberlite IRA-400(Cl^-)resin (Original resin), MCR, Pb^{2+} loaded MCR.

3.3.3. Distribution studies

3.3.3.1. Distribution coefficient (K_d) of metal ion

Movement/exchange of a particular metal ion, towards an ion exchanger, has been found to be dependent on (1) ion exchanger nature, (2) nature of background medium and (3) size and hydration of the metal ion [16]. The present exchange process can be interpreted in the light of above factors. K_d values, evaluated for all metal ions towards MCR, have been compiled in **Table 3.1 (**and also in **Figure 3.7)**. It has been observed that K_d value increases (up to 0.002 M) and then decreases as the metal ion concentration increases in the background solution (>0.002 to 0.007 M). The initial K_d value increase in lower concentration range may be due to availability of more exchangeable sites and hence responsible for nearly complete exchange of metal ions. Sufficient sites are not available at higher metal ion concentrations and hence the observed K_d value decreases. High K_d values are observed in the aqueous media of Co^{2+} (0.72 Å) and Pb^{2+} (1.44 Å) metal ion.

Table 3.1. Distribution coefficient (K_d) values (mL/g) with varying transition and heavy metal ions for MCR.

Metal ions	Ionic radii (A^0)	Distribution coefficient (K_d) values (mL/g) at different concentrations (M)						
		0.001M	0.002M	0.003M	0.004M	0.005M	0.006M	0.007M
Co^{2+}	0.72	164.7	212	128.81	105.55	91.66	64.7	39.13
Ni^{2+}	0.72	90.47	130.76	90.47	75	44.44	34.61	23.52
Cu^{2+}	0.74	104.54	122.22	80.55	45.45	34.86	34.4	28.57
Zn^{2+}	0.74	100	135.29	66.66	52.63	49.19	40	29.71
Cd^{2+}	0.97	114.28	214.81	100	64.70	50	42.85	38.46
Hg^{2+}	1.10	73.91	103.12	73.07	55.84	47.05	33.85	21.01
Pb^{2+}	1.44	133.33	341.17	91.66	63.15	43.93	39.88	36.58

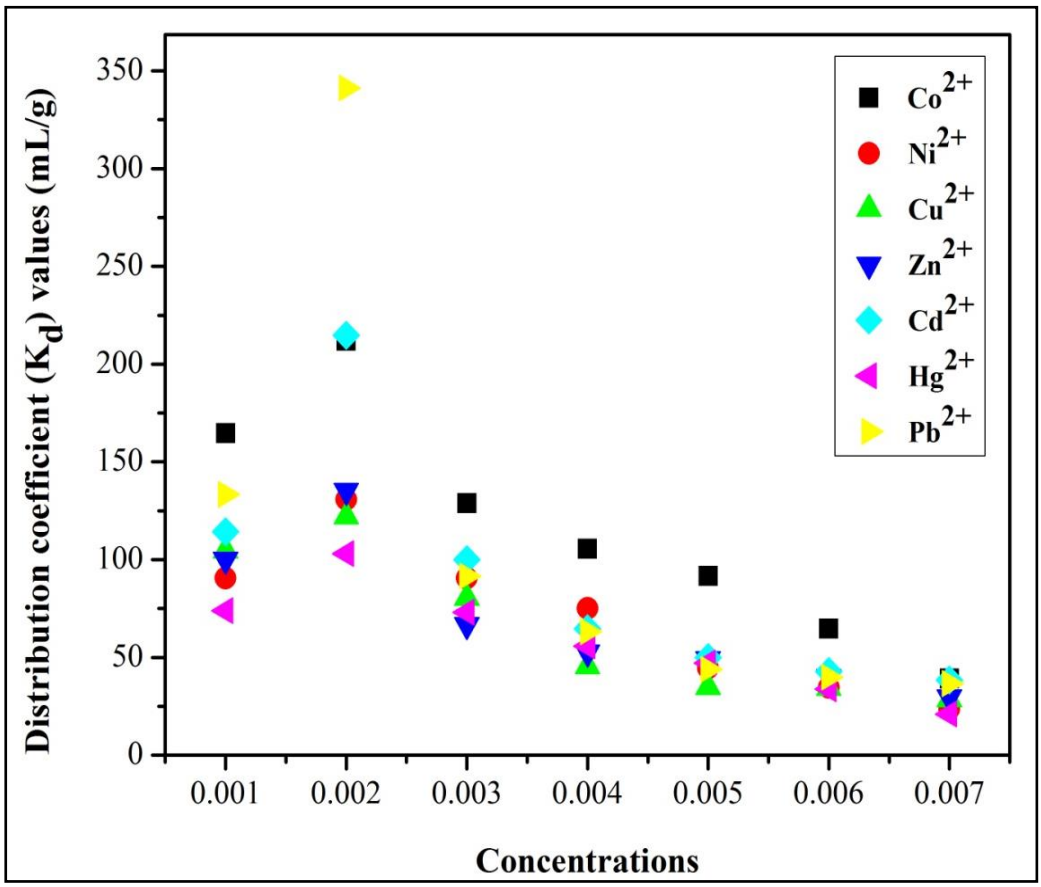

Figure 3.7. Effect of metal ion Co^{2+}, Ni^{2+}, Cu^{2+}, Zn^{2+}, Cd^{2+}, Hg^{2+} and Pb^{2+} for concentration vs. distribution coefficient (K_d) value.

Comparison of K_d data **(Table 3.2)** with earlier studies [26,31,32], performed with other types (cerium phosphate and modified cellulose) of exchangers/adsorbents, shows that the present MCR distinctly better, which may be due to the insertion of chelating moiety, which facilitates metal binding. K_d values determined for all metal ions under study, at optimum metal ion concentration (0.002 M) and in different electrolytic solutions (0.02 or 0.2 M), are given in **Table 3.2**. Further, K_d values in strong electrolytic media are lower as compared with weak electrolyte/aqueous media. The behavior is driven by increased ionic mobility and higher affinity of metal ion towards the exchanger compared with H^+ ions. It has been observed that the K_d values are lower in 0.2 M concentration of electrolyte, which can be understood in the light of competition between metal ion and electrolytic cation (H^+ or NH_4^+). Similar studies of metal ion exchange have also been performed with non-electrolyte (tert-butanol) [19]. In this study, K_d values were found to increase with increase in [(tert-butanol)] in the background solution. This suggests that nature and composition of electrolyte/non-electrolyte has a role to play in the mobility/exchange of metal ion towards exchanger.

Table 3.2. Distribution coefficient (K_d) values (mL/g) with different metal ions in various electrolyte media (0.02 M or 0.2 M).

Metal ions	Aqueous media	K_d values (mL/g) at different concentrations (M) in different electrolytes							
		NH_4NO_3		HNO_3		$HClO_4$		CH_3COOH	
		0.02 M	0.2 M	0.02 M	0.2 M	0.02 M	0.2 M	0.02 M	0.2 M
Co^{2+}	212	89.65	83.33	93.54	66.66	170.83	160	150	122.22
Ni^{2+}	130.76	124	89.65	77.41	57.14	103.44	83.33	120	100
Cu^{2+}	122.22	83.33	78.51	87.5	77	89.65	78.57	106.89	103.70
Zn^{2+}	135.29	122.22	110.71	100	89.65	103.70	87.5	113.79	100
Cd^{2+}	214.81	170.83	140	103.12	100	130.76	122.22	132.14	124.13
Hg^{2+}	103.12	100	96.96	45.16	40.62	71.42	66.66	83.33	87.5
Pb^{2+}	341.17	293.33	292.85	120	108.33	172.72	150	313.33	300

3.3.4. Adsorption studies

3.3.4.1. Effect of pH and contact time on the adsorption of metal ions

It is known that pH of the solution affects the solubility of metal ion and the competition ability with hydrogen ions. The sorption of transition and heavy metal ions was carried out in the pH range of 1.0 to 7.0 and data are shown in **Table 3.3**. Sorption data of all metal ions, at various pH, are also presented in **Figure 3.8**.

It can be seen in **Figure 3.8** that % uptake of metal ions increases with increase in the solution pH. At lower pH, percentage uptake of metal ions is also lower. This is because of the hydrogen competition of H^+ and metal ions for sorption/exchange sites. Experiments were not extended to above pH 7.0 because due to precipitation of all metal ions in the form of their hydroxides.

Table 3.3. Percentage uptake of metal ions with varying pH using MCR.

pH	Uptake of metal ion (%)						
	Co^{2+}	Ni^{2+}	Cu^{2+}	Zn^{2+}	Cd^{2+}	Hg^{2+}	Pb^{2+}
1	62.82	50	60	56.25	56.47	41.53	68
2	65.38	51.66	62.5	60	57.64	44.61	72
3	67.94	53.33	63.75	61.25	58.82	46.15	74.66
4	74.35	55	65	62.5	60	47.69	77.33
5	75.64	56.66	68.75	63.75	61.17	49.23	80
6	80.76	58.33	70	66.25	62.35	-	84
7	-	-	71.25	-	-	-	-

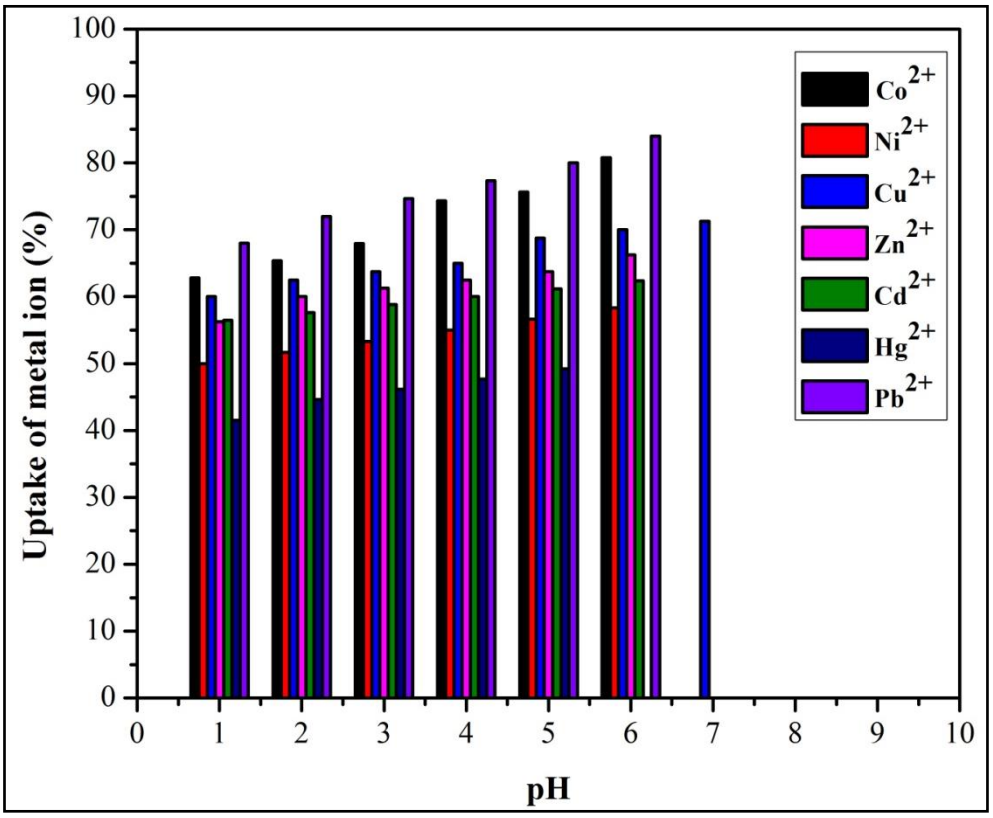

Figure 3.8. % Uptake of Co^{2+}, Ni^{2+}, Cu^{2+}, Zn^{2+}, Cd^{2+}, Hg^{2+} and Pb^{2+} metal ions vs. pH.

Contact time is one of the important parameters, which affect the adsorption. K_d increases with time (up to 120 min) and then show no further increase till 24 h **(Table 3.4)**. This implies that after saturation, it is difficult for the metal ion to adsorbed any more from the solution. This is due to the fact that initially maximum number of free sites are available (in the MCR) for adsorption of metal ions. However, occupancy of sites causes near saturation in ~120 min, **(**optimum time, see **Figure 3.12)** and a level of effect [33].

Table 3.4. Effect of contact time on the K_d value of metal ions using MCR.

Equilibrium values (mequie/g)										
Metal ions	15 min	30 Min	45 Min	60 min	75 min	90 min	105 min	120 min	135 min	150 min
Co^{2+}	0.86792	0.90566	0.92453	0.94340	0.95283	0.96226	0.97170	1	1	1
Ni^{2+}	0.73529	0.76471	0.77941	0.79412	0.82353	0.88235	0.94118	1	1	1
Cu^{2+}	0.77273	0.79545	0.84091	0.90909	0.93182	0.95455	0.97727	1	1	1
Zn^{2+}	0.88889	0.91111	0.92222	0.93333	0.95333	0.95556	0.97778	1	1	1
Cd^{2+}	0.89655	0.93103	0.93276	0.94828	0.95862	0.96552	0.98276	1	1	1
Hg^{2+}	0.87879	0.90909	0.92121	0.93939	0.95455	0.96970	0.98485	1	1	1
Pb^{2+}	0.70690	0.74138	0.75862	0.77586	0.81034	0.86207	0.94828	1	1	1

3.3.5. Adsorption isotherms

Adsorption isotherms are a critical piece of information on optimization of the use of adsorbents. Adsorption equilibrium isotherms provide fundamental physico-chemical information to evaluate the applicability of the adsorption process [12]. The relationship between the quantities of the metal ions adsorbed and the concentration equilibrium (C_e) can be obtained using the linear form of the Langmuir and Freundlich isotherm (most commonly used adsorption isotherm models).

The equilibrium isotherm data of metal ion adsorption can be described by linearized Langmuir adsorption isotherm expression (Eq. (7)).

$$\frac{C_e}{X/m} = \frac{1}{bV_m} + \frac{C_e}{V_m} \qquad (7)$$

where C_e (mg/g) is the amount of adsorbate adsorbed (at the equilibrium), X is the equilibrium concentration of adsorbate, m is the amount of adsorbent, while X/m represents q_e, V_m (mg/g) is the maximum monolayer adsorption capacity and b (dm^3/mg) is the Langmuir constant related to energy of adsorption and the affinity of the binding sites. A linear model of Langmuir isotherm was drawn by plotting C_e/q_e (g/L) vs. C_e (mg/L). These plots (with good correlation coefficient, R^2) result Langmuir constants, V_m and b (dimensionless). Langmuir constants, V_m and b (dimensionless), **Table 3.5** contains data for transition metal and heavy metal ions. **Figure. 3.9 (a and b)** show representative plots for Co^{2+} and Pb^{2+} and data for other metal ions are shown in **Figure 3.10 and Figure 3.11**. The separation factor R_L, used to predict favourability of the adsorption process, was calculated using the expression (Eq. (8)).

$$\mathbf{R_L} = \frac{\mathbf{1}}{\mathbf{(1 + bC_0)}} \tag{8}$$

where C_0 is the initial concentration of analytes. If $R_L < 1$, then the adsorption is favorable, while if $R_L > 1$ indicates unfavorable adsorption. However, $R_L = 1$ and $R_L = 0$ indicate linear adsorption and irreversible adsorption, respectively [26,34]. The Langmuir isotherm model resulted in a good fit of experimental adsorption (exchange) data **(Figure. 3.9 (a and b))**, which indicate that the model is appropriate for the sorption of all of the metal ions under study. Further, lower b values again confirm that the adsorption is favorable. V_m (maximum metal ion adsorption capacity of the exchanger), follows the order $Zn^{2+} > Ni^{2+} > Co^{2+} > Cu^{2+}$ among transition metal ions and $Pb^{2+} > Cd^{2+} > Hg^{2+}$ among heavy metal ions.

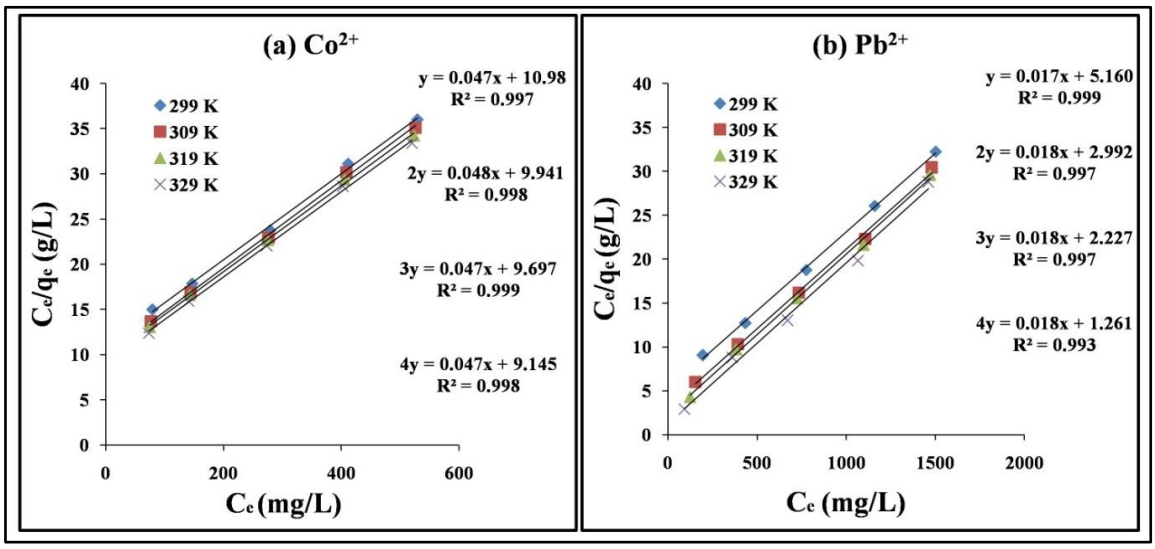

Figure 3.9. Langmuir adsorption isotherms of (a) transition metal ion (Co^{2+}) and (b) heavy metal ion (Pb^{2+}): 299 K, 309 K, 319 K and 329 K.

Table 3.5. Langmuir constants evaluated for transition and heavy metal ions using MCR.

Metal ions	Temperature (K)	Langmuir constants			
		R^2	b (dm^3/ mg)	V_m (mg/g)	R_L
Co^{2+}	299	0.997	0.0043	21.27	0.945
	309	0.998	0.0048	20.83	0.939
	319	0.999	0.0048	21.27	0.939
	329	0.998	0.0051	21.27	0.936
Ni^{2+}	299	0.996	0.0050	25.64	0.941
	309	0.997	0.0063	25.00	0.927
	319	0.985	0.0079	25.00	0.910
	329	0.971	0.0090	25.00	0.899
Cu^{2+}	299	0.948	0.0043	20.00	0.949
	309	0.945	0.0051	20.00	0.940
	319	0.942	0.0064	19.60	0.926
	329	0.986	00077	19.60	0.912
Zn^{2+}	299	0.981	0.0025	27.02	0.969
	309	0.987	0.0036	24.39	0.956
	319	0.997	0.0044	25.00	0.947
	329	0.996	0.0057	23.80	0.932
Cd^{2+}	299	0.997	0.0024	43.47	0.970
	309	0.998	0.0026	45.45	0.968
	319	0.999	0.0025	47.61	0.969
	329	0.999	0.0028	47.61	0.966
Hg^{2+}	299	0.957	0.0019	35.71	0.976
	309	0.963	0.0022	35.71	0.973
	319	0.968	0.0024	37.03	0.970
	329	0.972	0.0027	37.03	0.967
Pb^{2+}	299	0.999	0.0032	58.82	0.964
	309	0.997	0.0060	55.55	0.935
	319	0.997	0.0080	55.55	0.915
	329	0.993	0.0142	55.55	0.859

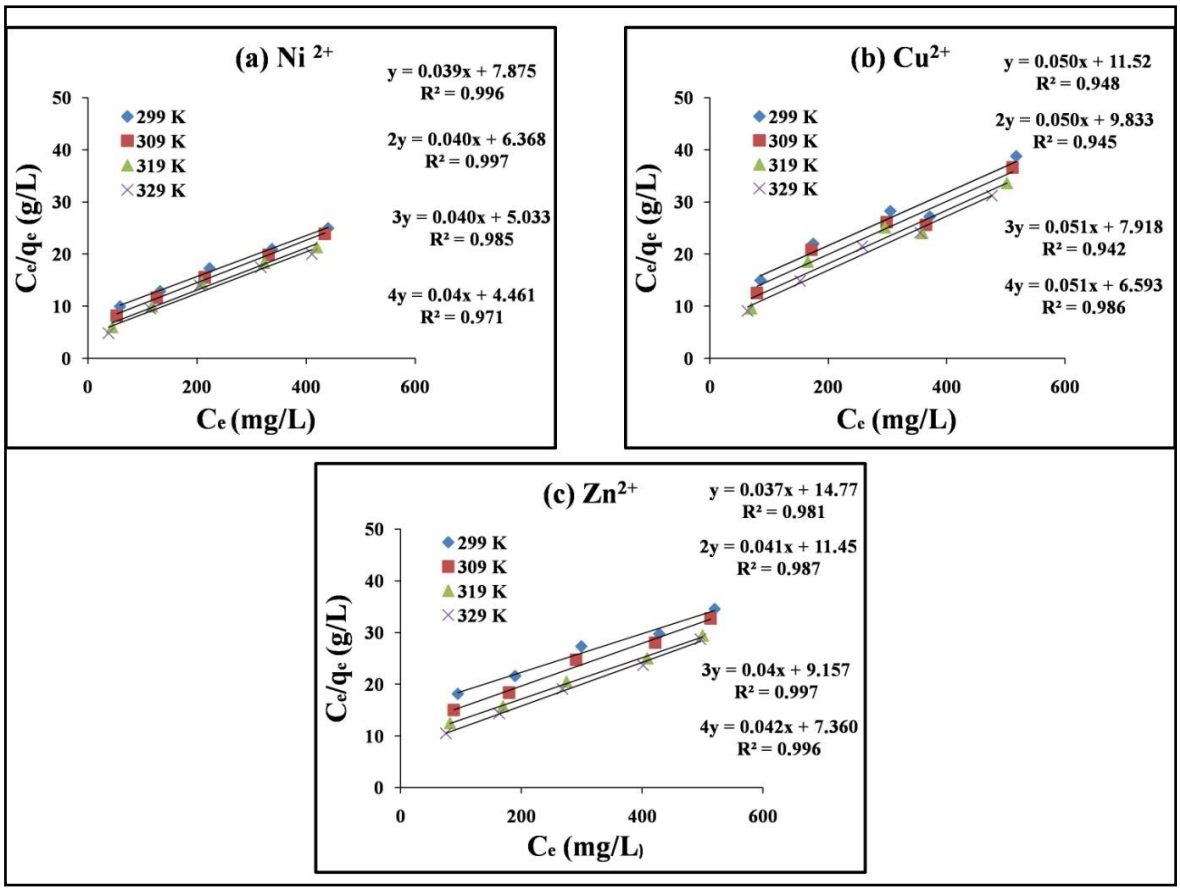

Figure 3.10. Langmuir adsorption isotherms of transition metal ion (a) Ni^{2+}, (b) Cu^{2+}, and (c) Zn^{2+}: 299 K, 309 K, 319 K and 329 K.

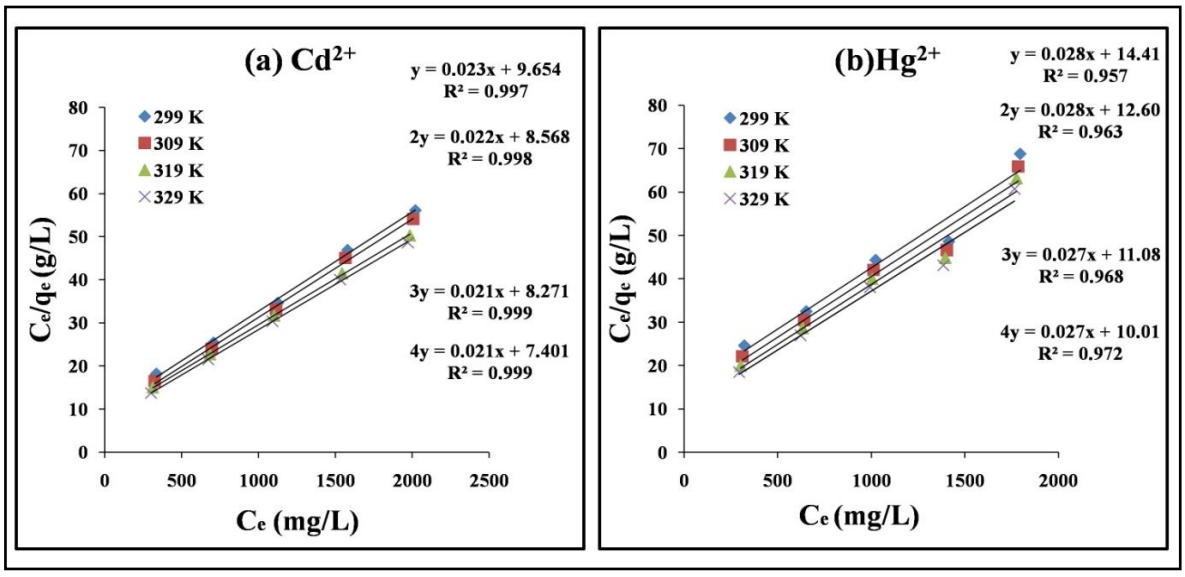

Figure 3.11. Langmuir adsorption isotherms of transition metal ion (a) Cd^{2+} and (b) Hg^{2+}: 299 K, 309 K, 319 K and 329 K.

3.3.6. Thermodynamic study of metal ion exchange process

In order to determine the basic thermodynamic parameters such as equilibrium constant (K), standard Gibbs free energy (ΔG°), standard enthalpy (ΔH°) and standard entropy (ΔS°) changes, exchange was studied at different temperatures (299–329 K). Thermodynamic parameters are used to support the nature of the adsorption process proposed above. The calculated values of thermodynamic parameters are given in **Table 3.6**. Further, equilibrium studies for metal-loaded MCR were apparently attained within 120 min. A plot between **(Figure 3.12)** fractional attainment of equilibrium, U(t) vs. time (t) gives idea of equilibrium saturation for each metal ion.

Table 3.6. Thermodynamic parameters evaluated for M^{2+}-H^{+} exchange at various temperatures using MCR.

Metal ions	Temperature (K)	K	ΔG° (kJ/mol)	ΔH° (kJ/mol)	ΔS° (J/mol/°C)
Co^{2+} -H^{+}	299	2.14	-0.94	22.33	77.85
	309	2.18	-1.00		75.52
	319	2.25	-1.08		73.39
	329	2.32	-1.15		71.38
Ni^{2+} -H^{+}	299	1.96	-0.83	15.77	55.54
	309	1.98	-0.88		53.89
	319	2.05	-0.95		52.42
	329	2.07	-1.00		50.97
Cu^{2+} -H^{+}	299	2.28	-1.02	34.22	117.88
	309	2.45	-1.15		114.48
	319	2.49	-1.21		111.08
	329	2.59	-1.30		107.99
Zn^{2+} -H^{+}	299	2.11	-0.93	25.06	86.93
	309	2.23	-1.03		84.44
	319	2.24	-1.06		81.91
	329	2.33	-1.15		79.68
Cd^{2+} -H^{+}	299	2.00	-0.86	25.97	89.78
	309	2.09	-0.95		87.14
	319	2.18	-1.03		84.67
	329	2.21	-1.08		82.26
Hg^{2+} -H^{+}	299	2.27	-1.02	17.64	62.41
	309	2.29	-1.06		60.54
	319	2.39	-1.15		58.93
	329	2.42	-1.21		57.30
Pb^{2+} -H^{+}	299	2.19	-0.97	36.85	126.52
	309	2.28	-1.06		122.70
	319	2.42	-1.17		119.22
	329	2.51	-1.26		115.85

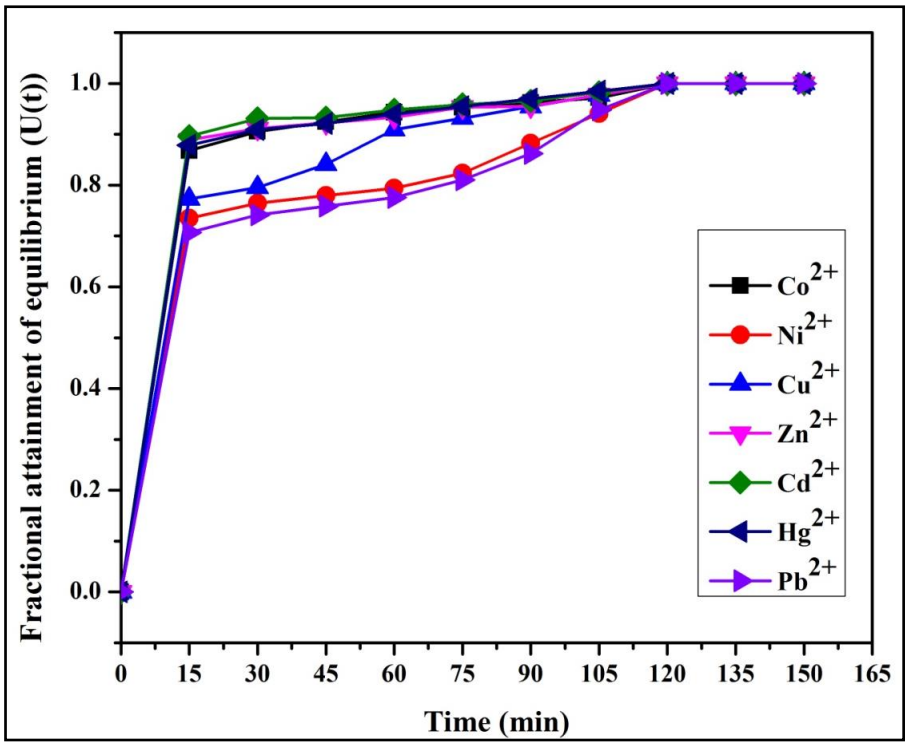

Figure 3.12. Fractional attainment of equilibrium for varying metal ions vs. time using MCR.

K increases with increasing temperature for transition and heavy metal ions. This indicates higher affinity of metal ion to the exchanger at higher temperature, which reveals endothermicity of ion exchange process. The value of ΔG° is negative and decrease with increase in temperature. The negative ΔG° value means that all metal ion sorption onto the MCR and process favoured with increasing temperature. This confirms that exchange process is feasible and spontaneous in nature. At any given temperature, high negative ΔG° value for Cu^{2+} and Hg^{2+} indicate ease of exchange for these metal ions. The parameters are driven by hydration of metal ions (less ΔG° values is related to more hydrated metal ion and vice versa). ΔH° was positive in all cases, indicating that the process is endothermic in nature. The order of enthalpy change for transition metal ions ($Cu^{2+} > Zn^{2+} > Co^{2+} > Ni^{2+}$) and heavy metal ions ($Pb^{2+} > Cd^{2+} > Hg^{2+}$) can be related to hydrated ion size. Higher/positive values of ΔH° indicate more endothermicity of the exchange process and the requirement of more energy for dehydration. The higher ΔS° values for Cu^{2+} and Pb^{2+} attributed to greater dehydration (which indicates greater disorder produced) during the exchange [35].

3.3.7. Adsorption kinetics

The kinetics of the adsorption of various metal ions (transition and heavy metal) using MCR was studied by observing q_t at varied contact time (t). To investigate the adsorption process of the metal ion on MCR, the pseudo-first-order, pseudo-second-order, and intraparticle diffusion models were used **(**Eqs. (3)–(5); see **Figure 3.13 (a-c))**. Kinetic parameters are shown in **Table 3.7**. **Figure 3.13** shows typical kinetics of adsorption for Zn^{2+} and Cd^{2+} ions. It can be observed that the adsorption of metal ion onto MCR was rapid in the first 15 min and then reached an equilibrium gradually in 120 min. Analysis of data shows distant R^2 values from 1 suggesting that pseudo-first-order is not applicable. However pseudo-second-order equation results **(Table 3.7)** matching of q_e (cal) and q_e (exp) together with a good correlation coefficient (Zn^{2+} = 0.998 and Cd^{2+} = 0.999). This suggests the validity of pseudo-second-order kinetics for adsorption process. The kinetic data were also evaluated by intraparticle diffusion Weber–Morris model. A plot of qt vs. the square root of time ($t^{1/2}$) is linear if intraparticle diffusion is involved in the adsorption process. Further, such linear plots should pass through the origin. R^2 value (Zn^{2+} = 0.960 and Cd^{2+} = 0.964) and the absence of passing the straight line through the origin hint that the intraparticle diffusion model is not valid to explain present adsorption kinetics. All kinetic model graphs are shown in **Figure 3.14 (a-c)** and **Figure 3.15 (a-c)**. On the basis of above discussion, adsorption of transition and heavy metal ion follows a pseudo-second-order reaction pathway [36,37].

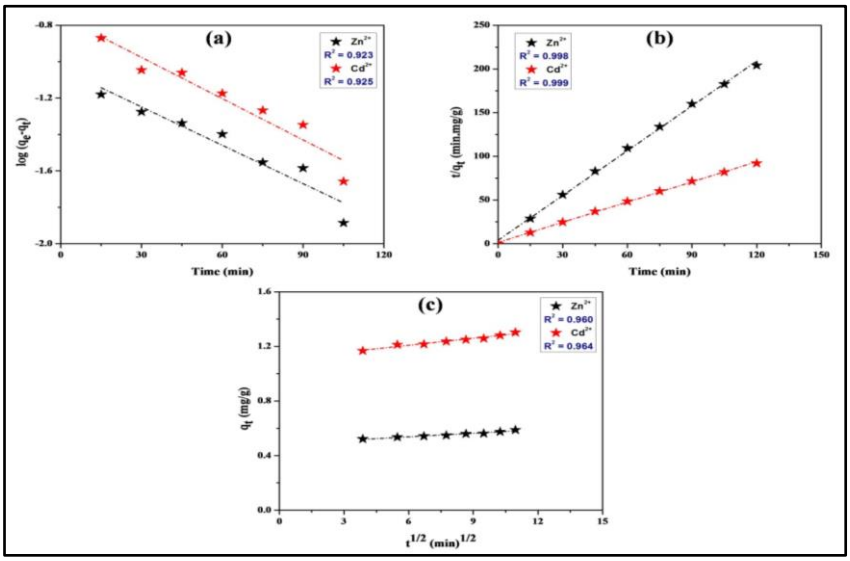

Figure. 3.13. (a) Pseudo-first-order kinetics, (b) Pseudo-second-order kinetics, and (c) Intraparticle diffusion model for adsorption of transition metal ion (Zn^{2+}) and heavy metal ion (Cd^{2+}) on MCR.

Table 3.7. Kinetic parameters of metal ion adsorption onto MCR conditions: 0.1 g adsorbent over 0.002 M at optimum conditions of other variables.

Models	Parameters	Co^{2+}	Ni^{2+}	Cu^{2+}	Zn^{2+}	Cd^{2+}	Hg^{2+}	Pb^{2+}
Pseudo first order	K_1	0.0161	0.0138	0.0253	0.0161	0.0161	0.0207	0.0138
	q_e (cal)	0.0995	0.0942	0.0963	0.0888	0.0958	0.0882	0.0937
	R^2	0.9249	0.9178	0.9217	0.9023	0.9119	0.9001	0.9167
Pseudo second order	K_2	0.874	0.618	0.522	0.768	0.261	0.571	0.687
	q_e (cal)	0.8613	0.7808	0.7509	0.8063	0.6416	0.7604	0.8007
	R^2	0.9996	0.9995	0.9995	0.9996	0.9992	0.9995	0.9995
Interparticle diffusion	K_{id}	0.010	0.017	0.019	0.008	0.017	0.022	0.116
	C	0.504	0.195	0.348	0.485	1.105	1.076	1.037
	R^2	0.975	0.943	0.976	0.960	0.964	0.993	0.945
Experimental	q_e (exp)	0.624	0.398	0.558	0.588	1.303	1.323	2.403

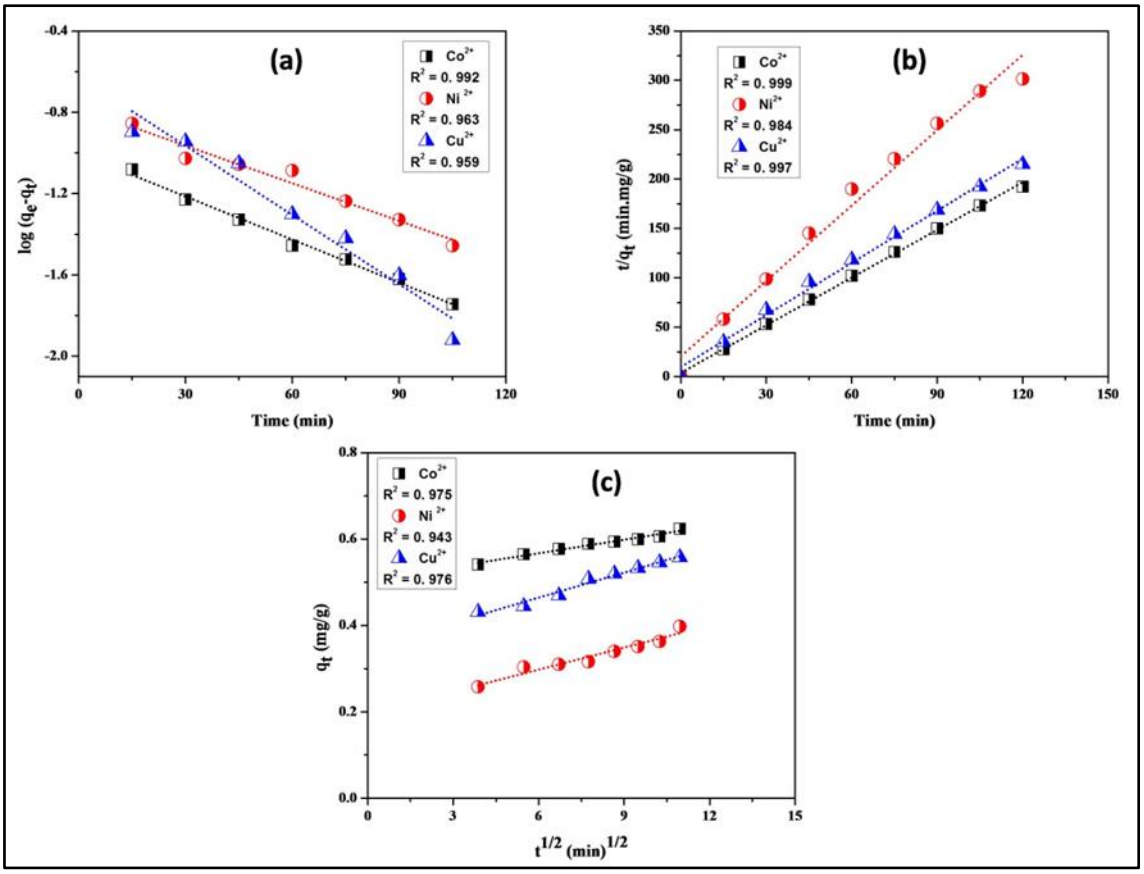

Figure. 3.14. (a) Pseudo-first-order kinetics, (b) Pseudo-second-order kinetics, and (c) Intraparticle diffusion model for adsorption of transition metal (Co^{2+}, Ni^{2+}, Cu^{2+}) on MCR.

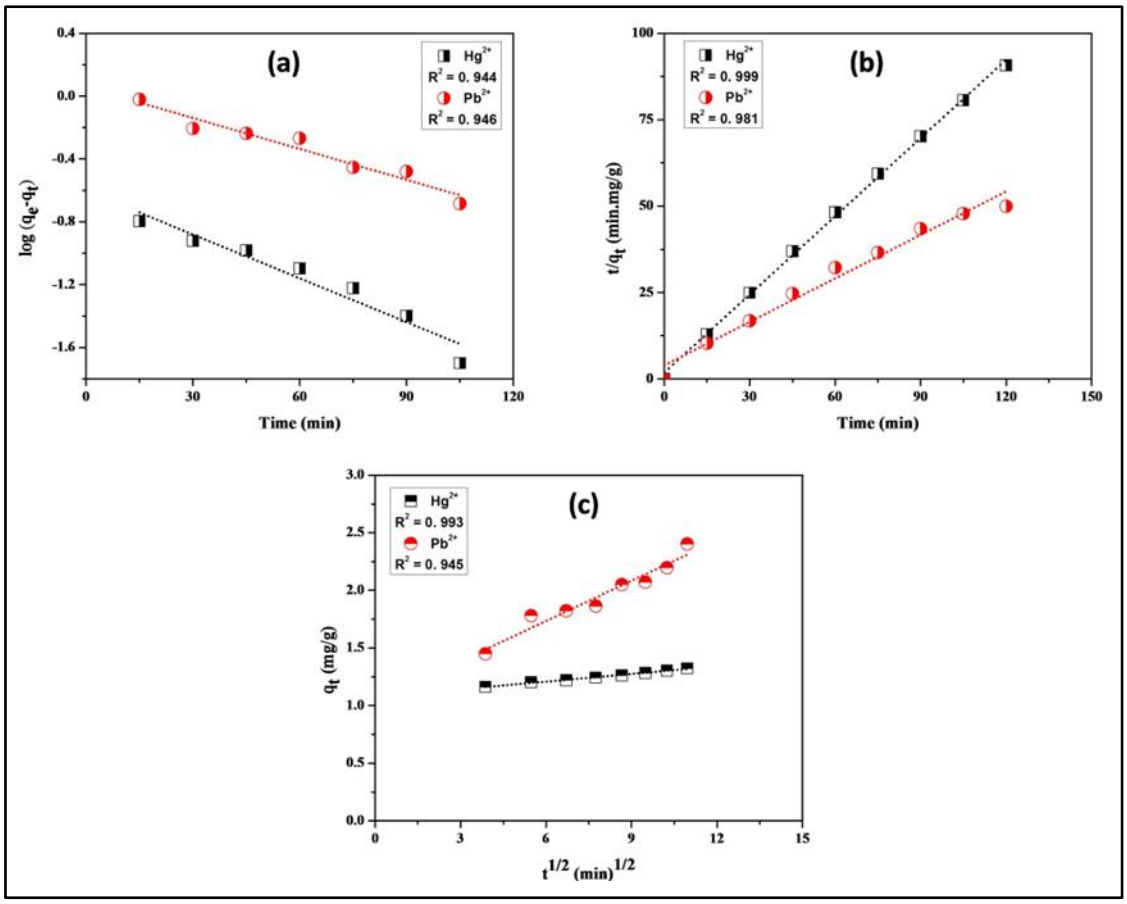

Figure. 3.15. (a) Pseudo-first-order kinetics, (b) Pseudo-second-order kinetics, and (c) Intraparticle diffusion model for adsorption of heavy metal (Hg^{2+} and Pb^{2+}) on MCR.

3.3.8. Effect of nature of eluent

The elution behavior **(Table 3.8)** of transition and heavy metal ions (Co^{2+}, Ni^{2+}, Cu^{2+}, Zn^{2+}, Cd^{2+}, Hg^{2+} and Pb^{2+}) have been performed using different electrolytes (ammonium nitrate, perchloric acid, glacial acetic acid, and nitric acid). Eluent data of **Table 3.8** shows that 0.2 M HNO_3 is a better eluent among others. Using 0.2 M HNO_3, order of the percentages of metal eluted among the transition metal ions was $Co^{2+} > Cu^{2+} > Ni^{2+} > Zn^{2+}$ and that among the heavy metal ions was $Hg^{2+} > Cd^{2+} > Pb^{2+}$. The % metal eluted in all cases is in the range of 60%–96%. K_d value indicate that Co^{2+} and Hg^{2+} metal ion exchanges more and hence less eluted as shown in **Figure. 3.16** (for Co^{2+}) and **Figure. 3.17** (for Hg^{2+}) [38]. All other metal's graph is shown in **Figure. 3.18** – **Figure. 3.22**.

Table 3.8. Percentage elution (% E) of metal ions in different electrolyte media using MCR.

Metal ions	Percentage elution (% E) of metal ions in different electrolyte media							
	NH_4NO_3		HNO_3		$HClO_4$		CH_3COOH	
	0.02 M	0.2 M	0.02 M	0.2 M	0.02 M	0.2 M	0.02 M	0.2 M
Co^{2+}	62.47	69.41	81.83	91.62	69.41	70.80	69.41	76.35
Ni^{2+}	62.93	68.48	83.29	88.85	74.03	77.74	68.48	74.03
Cu^{2+}	67.16	70.28	82.78	90.60	79.66	85.91	71.85	78.10
Zn^{2+}	69.20	72.09	80.72	86.51	61.99	73.51	72.07	74.96
Cd^{2+}	60.30	63.00	90.35	91.77	68.36	75.30	79.47	82.16
Hg^{2+}	60.00	64.00	92.00	96.00	70.00	74.00	84.00	88.00
Pb^{2+}	61.22	63.02	88.23	90.03	70.24	72.02	77.43	81.04

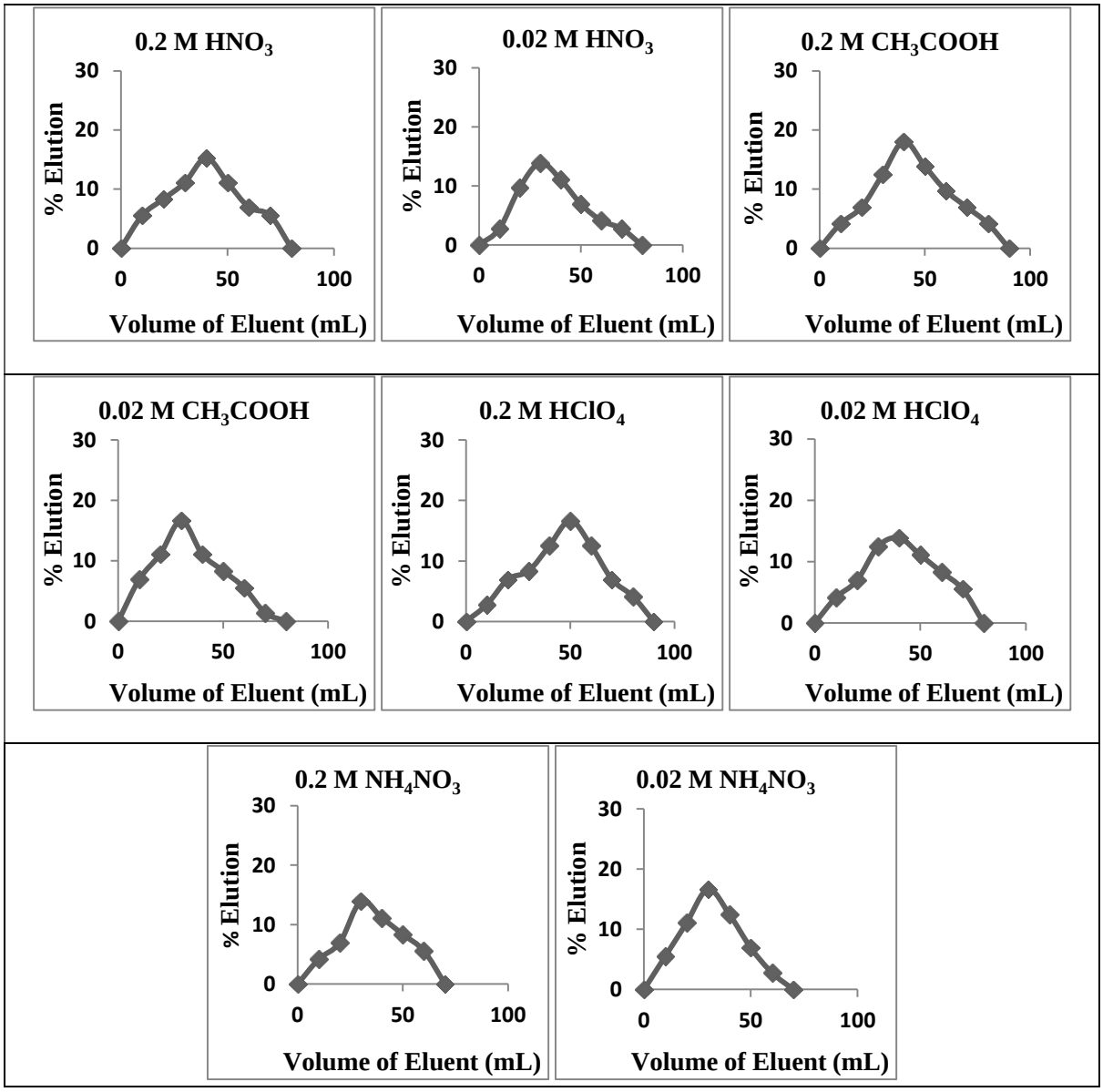

Figure. 3.16. Elution curve of Co^{2+} using MCR.

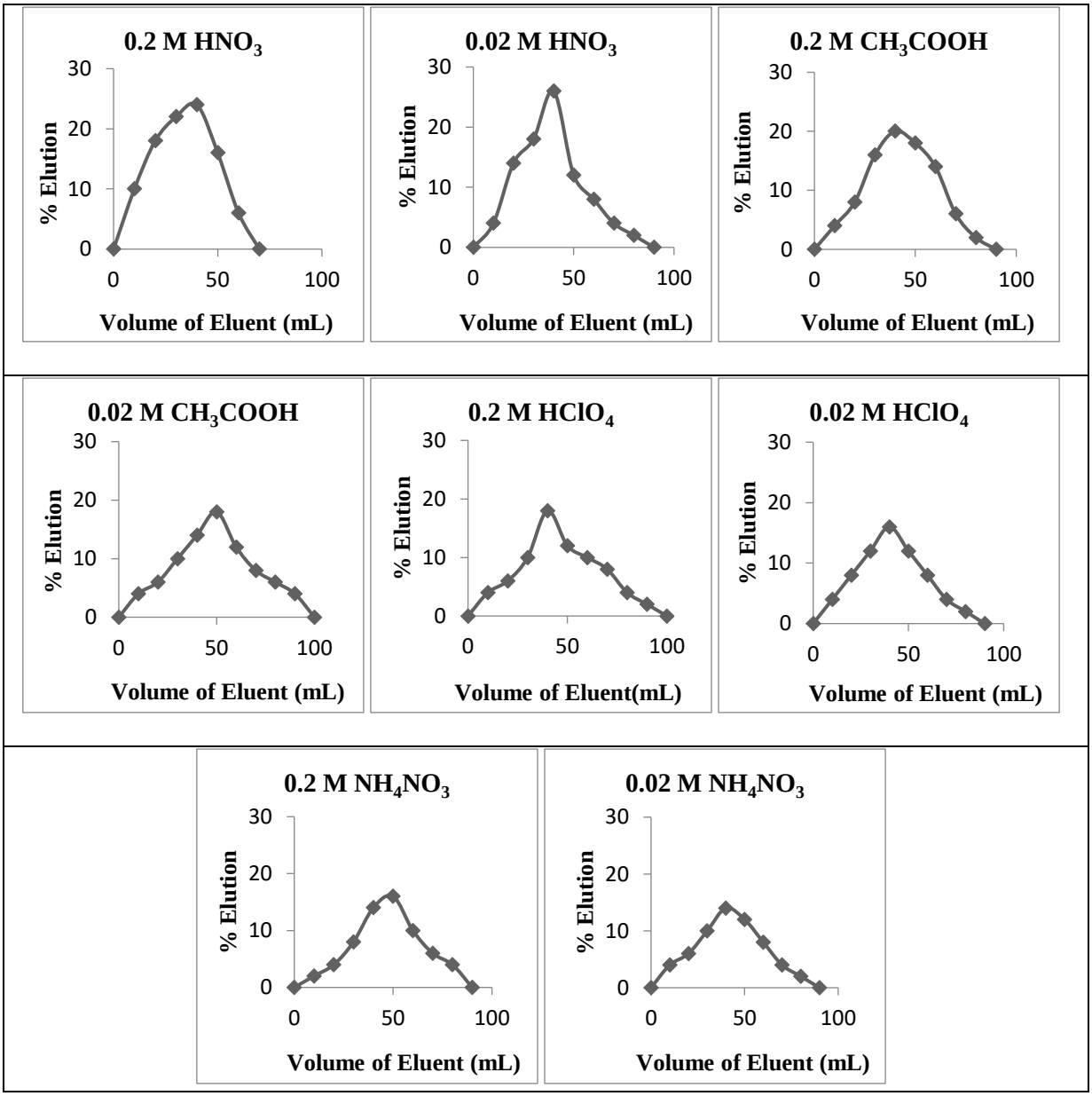

Figure. 3.17. Elution curve of Hg^{2+} using MCR.

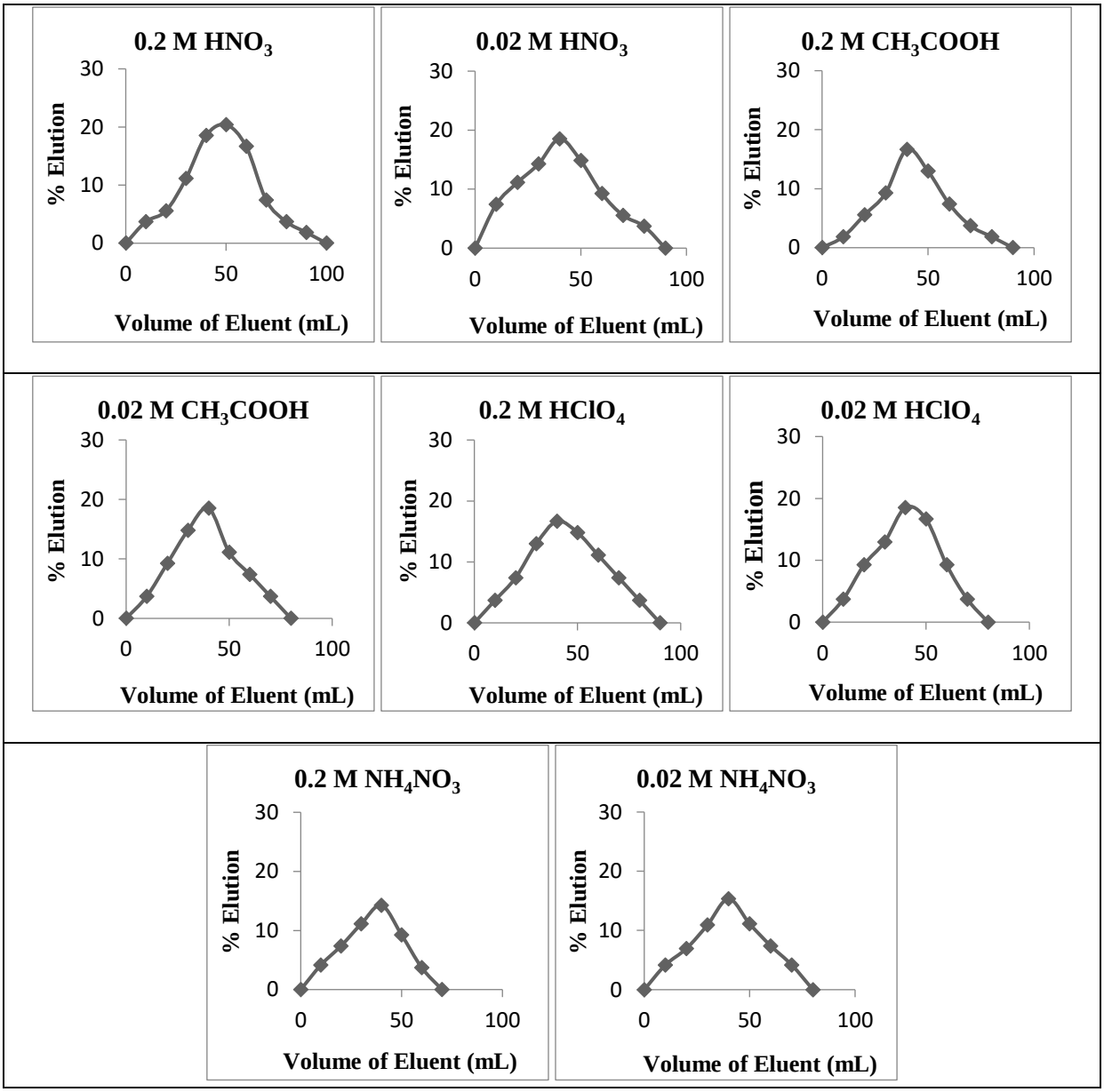

Figure. 3.18. Elution curve of Ni^{2+} using MCR.

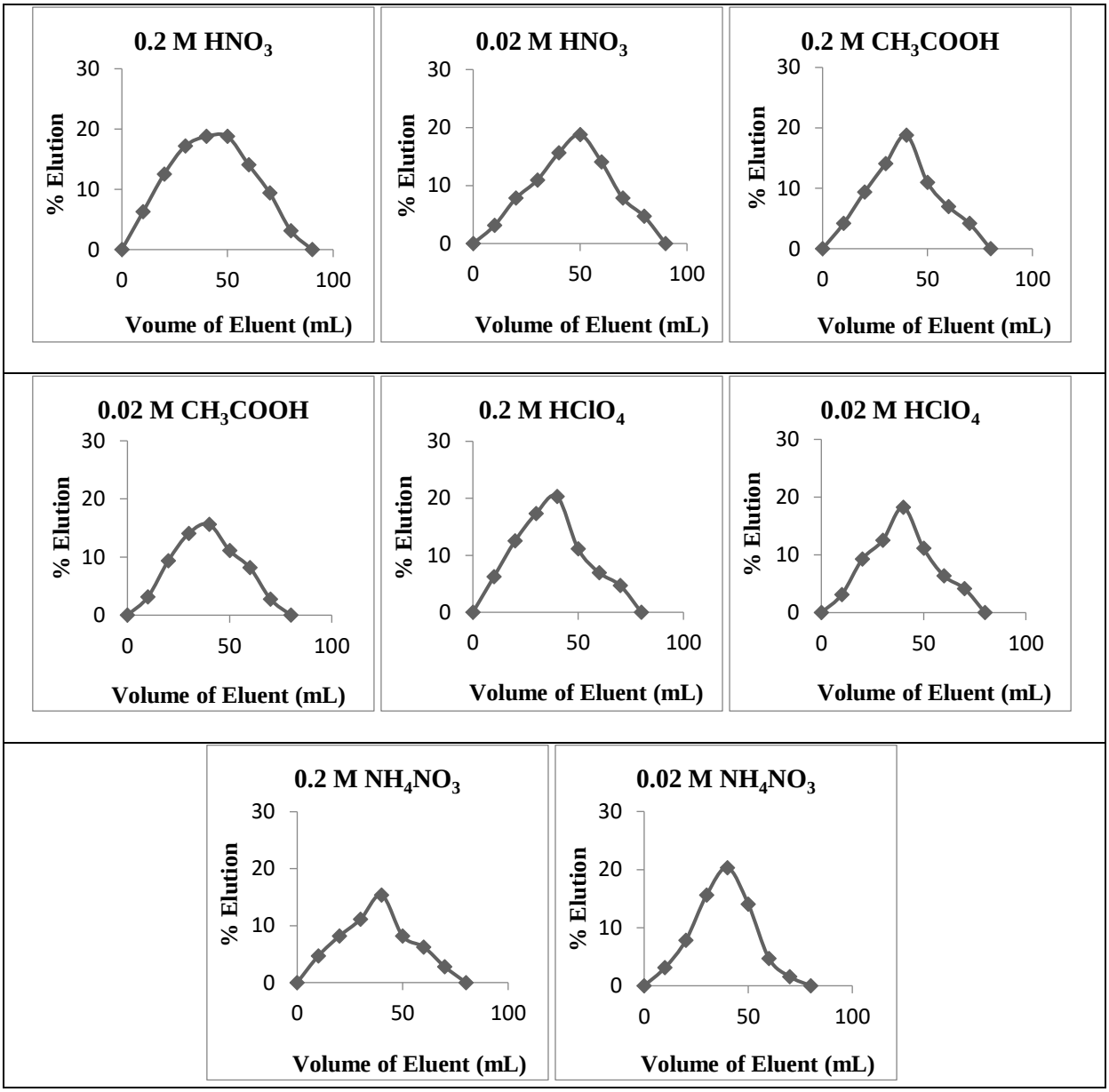

Figure. 3.19. Elution curve of Cu^{2+} using MCR.

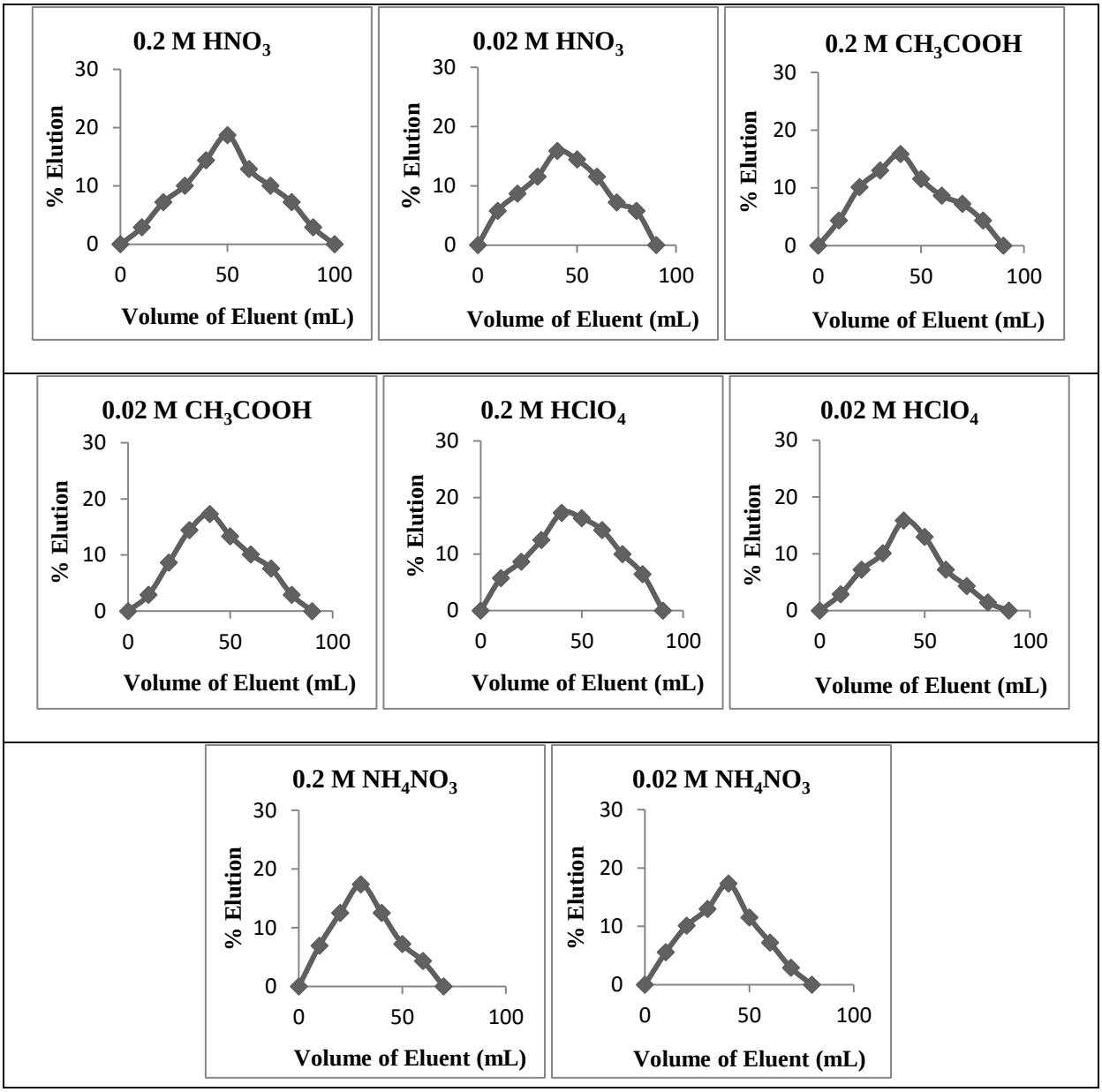

Figure. 3.20. Elution curve of Zn^{2+} using MCR.

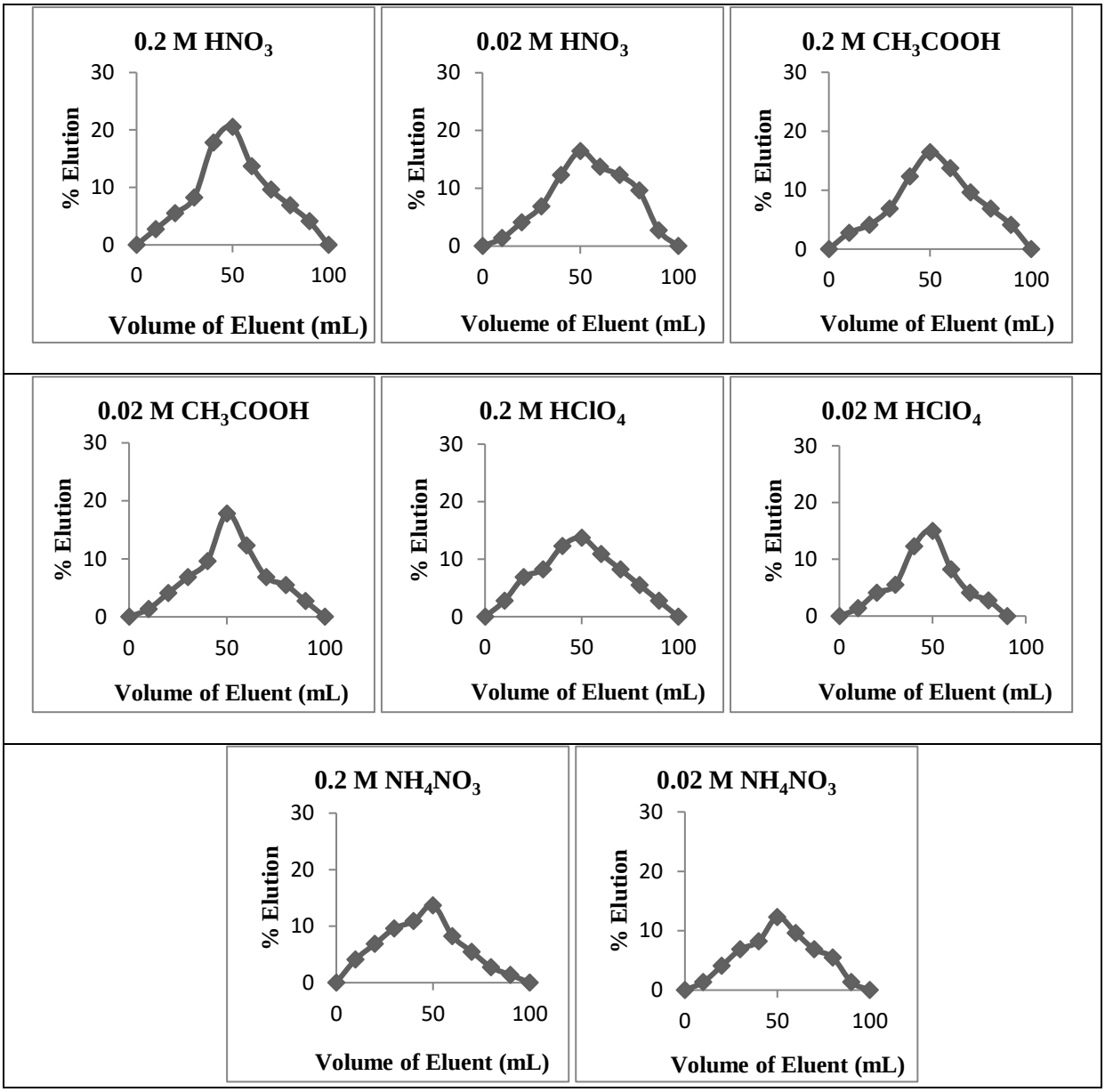

Figure. 3.21. Elution curve of Cd^{2+} using MCR.

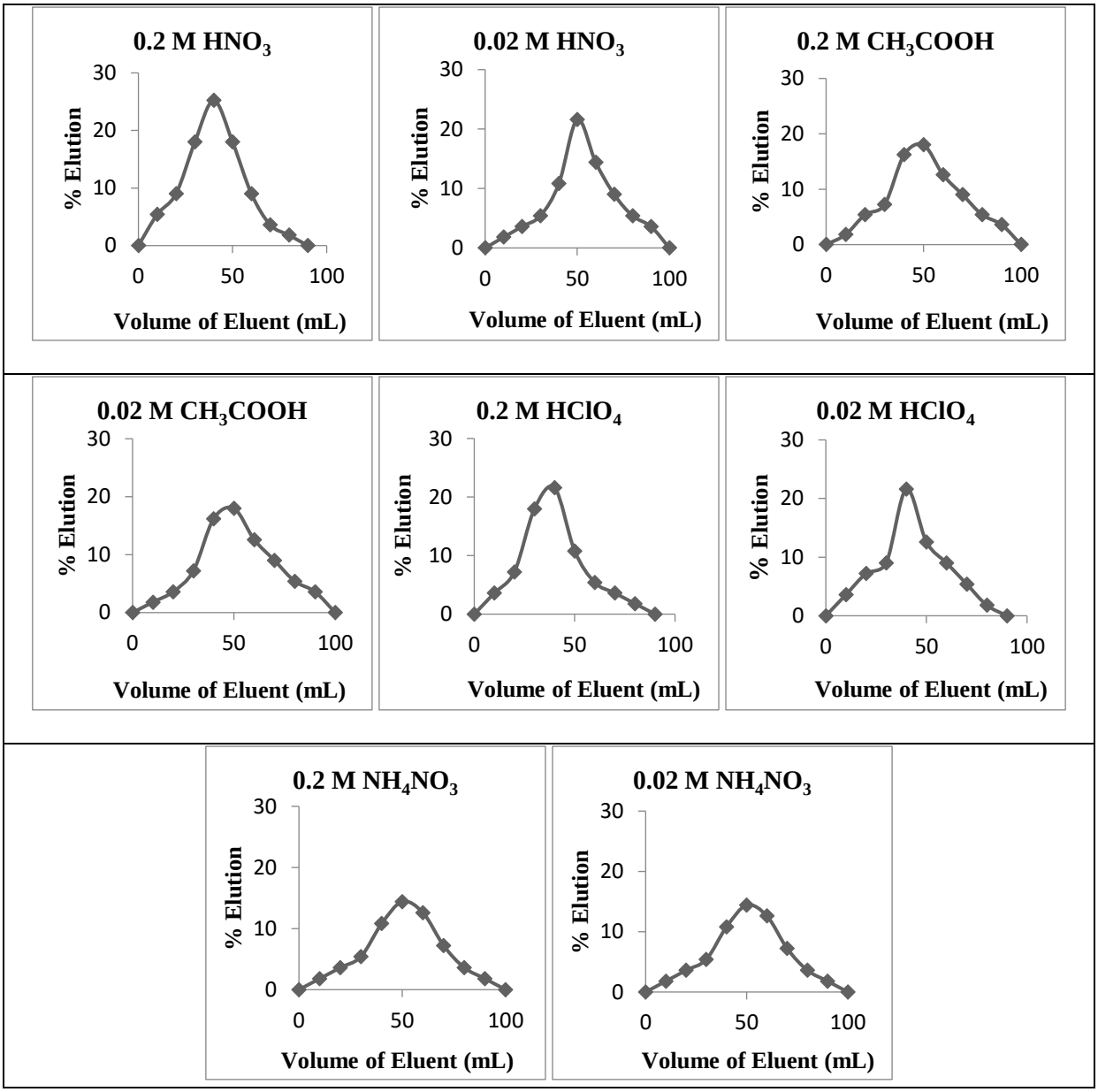

Figure. 3.22. Elution curve of Pb^{2+} using MCR.

3.4. Conclusions

Amberlite IRA-400(Cl^-) resin has been modified (MCR) with disodium salt of EDTA. The MCR has been characterized by FTIR, EDX and SEM analysis and then used for the removal of metal ions from aqueous solution. Distribution coefficient (K_d) has been determined in aqueous or electrolytic solution for metal ion exchange. K_d values, at different time interval are used to evaluate fractional attainment of equilibrium. Effect of pH has been studied for the metal ion exchange process.

The transition and heavy metal ions were adsorbed onto the MCR in a monolayer of adsorption as confirmed by applying Langmuir model. The adsorption mechanism of transition metal ion (Cu^{2+}) and heavy metal ion (Pb^{2+}) onto the MCR has been found endothermic as indicated from the higher positive value of ΔH°. The higher negative value of ΔG° and positive value of ΔS° indicates the spontaneity of the metal ion exchange process. Adsorption data, with time, have been fitted well in pseudo-second-order kinetic model. Metal ion exchange process, developed have by using MCR, can be more effective than the other methods reported in the literature [26,31,32].

3.5. References

[1] N.L. Nemerow, A. Dasgupta, Ind. and Hazard Waste Treat., Van Nostrand Reinhold, New York, 1991, pp. 378.

[2] I. Ali, Chem. Rev. **112** (2012) 5073−5091.

[3] A.M. Elbedwehy, A.M. Abou-Elanwar, A.O. Ezzat, A.M. Atta, Polymers **11** (2019) 1938.

[4] R. Kumar, S.K. Jain, R.K. Misra, M. Kachchwaha, P.K. Khatri, Int. J. Environ. Sci. Technol. **9** (2012) 79–84.

[5] J. Aguado, J.M. Arsuaga, A. Arencibia, M. Lindo, V. Gascon, J. Hazard. Mater. **163** (2009) 213–221.

[6] Z.A. ALOthman, Inamuddin, Mu. Naushad, J. Inorg. Organomet. Polym. **23** (2013) 257–269.

[7] G. Zhou, J. Luo, C. Liu, L. Chu, J. Crittenden, Water Res. **131** (2018) 246–254.

[8] R. Kumar, M.A. Barakat, Y.A. Daza, H.L. Woodcock, J.N. Kuhn, J. Colloid. Int. Sci., **408** (2013) 200–205

[9] L.T. Friberg, G.F. Nordberg, B.A. Fowler, M. Nordberg, Handbook on the Toxicology of metals, Elsevier, Amsterdam, The Netherlands, 1979.

[10] M.E. Mahmoud, A.A. Yakout, H. Abdel-Aal, M.M. Osman, Bio. Res. Technol. **106** (2012) 125−132.

[11] M. Mohamed, E. Soliman, A. Dlssouky, Analyt. Sci. **13** (1997) 765−769.

[12] S. Zhang, X. Li, J.P. Chen, Carbon **48** (2010) 60–67.

[13] E.S. Dragan, M.V. Dinu, D. Timpu, Bio. Res. Technol. **101** (2010) 812–817.

[14] W. Peng, H. Li, Y. Liu, S. Song, J. Mol. Liq. **230** (2017) 496–504.

[15] T.G. Kebede, S. Dube, M.M. Nind, J. Environ. Sci. Health, Part A, **54** (2019) 337–351.

[16] B. Shah, U. Chudasama, Sep. Sci. Technol. **54** (2019) 1560–1572.

[17] S. Sun, A. Wang, Sep. Purif. Technol. **51** (2006) 409–415.

[18] S. Kocaoba, Adsorpt. Sci. Technol. **21** (2003) 831–840.

[19] M.A. Ali, M.A. Rahman, A.M. Shafiqul Alam, Anal. Chem. Lett. **3** (2013) 199–207.

[20] J.N. Mathur, P.K. Khopkar, Ion. Exch. Lett. **3** (1985) 653.

[21] P. Kampalanonwat, P. Supaphol, Appl. Mater. Interface **2** (2010) 3619–3627.

[22] B.L. Rivas, S. Villegas, B. Ruf, J. Appl. Poly. Sci. **99** (2006) 3266–3274.

[23] C. Liu, R. Bai, L. Hong, J. Colloid Interface Sci. **303** (2006) 99–108.

[24] S.S. Kalaivani, V. Thangaraj, M. Arukkani, V.T. Kadathur, A. Dhanasekaran, S. Sivanesan, L. Ravikumar, Water Res. Ind. **5** (2014) 21–35.

[25] P. Patel, U. Chudasama, Ion. Exch. Lett. **4** (2011) 7–15.

[26] T. Parangi, B. Wani, U. Chudasama, Desal. Wat. Treat. **57** (2015) 1–9.

[27] S. Nethaji, A. Sivasamy, A.B. Mandal, Int. J. Environ. Sci. Technol. **10** (2013) 231–242.

[28] S. Lagergren, Handl. Band. **24** (1898) 1–39.

[29] Y.S. Ho, G. McKay, J. Proc. Biochem. **34** (1999) 451–465.

[30] W.J. Weber, J.C. Morris, Adsorption Processes for Water Treatment, Butterworth, London, 1987.

[31] T. Parangi, B. Wani, U. Chudasama, Desalin. and Water Treat. **38** (2012) 126–134.

[32] R. Saravanan, R. Mahalakshmi, M.S. Karthikeyan, L. Ravikumar, Water Sci. Technol. **80** (2019) 1549–1561.

[33] S. Xiuling, D. Huipu, S. Liu, Q. Hui, J. Chem. **2014** (2014) 5.

[34] W. Li, Q. Liu, J. Liu, H. Zhang, R. Li, Z. Li, X. Jing, J. Wang, Appl. Surf. Sci. **403** (2017) 378–388.

[35] R. Kunin, J. Am. Pharm. Assoc. **47** (1958) 836.

[36] S. Sinha, S.S. Behera, S. Das, A. Basu, R.K. Mohapatra, B.M. Murmu, N.K. Dhal, S.K. Tripathy, P.K. Parhi, Chem. Eng. Commun. **205** (2018) 2–12.

[37] I.M. Ali, M.Y. Nassar, Y.H. Kotp, M. Khalil, Part. Sci. Technol. **37** (2019) 207–219.

[38] P. Patel, U. Chudasama, Sep. Sci. Technol. **46** (2011) 1346–1347.